Efficient generation of stable bispecific IgG1 by controlled Fab-arm exchange

Aran F. Labrijn[a], Joyce I. Meesters[a], Bart E. C. G. de Goeij[a], Ewald T. J. van den Bremer[a], Joost Neijssen[a], Muriel D. van Kampen[a], Kristin Strumane[a], Sandra Verploegen[a], Amitava Kundu[b], Michael J. Gramer[b], Patrick H. C. van Berkel[a,1], Jan G. J. van de Winkel[a,c], Janine Schuurman[a], and Paul W. H. I. Parren[a,2]

[a]Genmab, 3584 CM, Utrecht, Netherlands; [b]Genmab, Brooklyn Park, MN 55445; and [c]Immunotherapy Laboratory, Department of Immunology, University Medical Center, 3508 GA, Utrecht, Netherlands

Edited by Michel C. Nussenzweig, The Rockefeller University, New York, NY, and approved February 19, 2013 (received for review November 21, 2012)

The promise of bispecific antibodies (bsAbs) to yield more effective therapeutics is well recognized; however, the generation of bsAbs in a practical and cost-effective manner has been a formidable challenge. Here we present a technology for the efficient generation of bsAbs with normal IgG structures that is amenable to both antibody drug discovery and development. The process involves separate expression of two parental antibodies, each containing single matched point mutations in the CH3 domains. The parental antibodies are mixed and subjected to controlled reducing conditions in vitro that separate the antibodies into HL half-molecules and allow reassembly and reoxidation to form highly pure bsAbs. The technology is compatible with standard large-scale antibody manufacturing and ensures bsAbs with Fc-mediated effector functions and in vivo stability typical of IgG1 antibodies. Proof-of-concept studies with HER2×CD3 (T-cell recruitment) and HER2×HER2 (dual epitope targeting) bsAbs demonstrate superior in vivo activity compared with parental antibody pairs.

immunotherapy | pharmacokinetics | anti-tumor

The prototypic monoclonal antibody (mAb) used in human therapy contains two identical antigen-combining sites and thus binds monospecifically and bivalently. Due to the multifactorial nature of certain diseases, however, not all patients respond adequately to monospecific antibody therapy. This heterogeneity is one of the main reasons why antibodies containing two distinct binding specificities, i.e., bispecific antibodies (bsAbs), are thought to have great potential as dual-targeting therapeutic agents, as also illustrated by the expanding number of bsAb-based formats in development (1). However, the general application of most of these formats for therapeutic use has been hampered by shortcomings with respect to physicochemical stability, pharmacokinetic properties, immunogenicity, and scalability of manufacturing and purification (2–4). Furthermore, the inherent design of most bsAb-based formats precludes efficient screening of large numbers of bispecific combinations or requires reengineering on final candidate selection (5).

As each antigen-combining site is formed by the variable domains of both heavy (H) and light (L) chains, VH and VL, respectively, one of the initial challenges in bsAb development (quadromas coexpressing two H and two L chains) was in obtaining sufficient yield of the functional bsAb from the mixture of 10 possible H_2L_2 combinations (6). Since then, strategies to circumvent H-L chain mispairing [e.g., common L chain (7), species-restricted H-L chain pairing (8), crossover of CL and CH1 domains (9)] in combination with strategies to promote heterodimerization of the two H chains [e.g., "knobs-into-holes" (7), electrostatic steering (10), strand-exchange engineered domains (SEED) (11)] have increased homogeneity and yield of the desired end product (2). Alternatively, approaches using additional VH-VL pairs (12), single-chain (sc)Fv (13–16), or domain antibody (dAb) (17, 18) fragments for target binding allow incorporation of multiple antigen-combining sites in a single polypeptide chain (or single HL pair), which also increases product homogeneity and yield, although often at the expense of the physicochemical and/or pharmacokinetic properties of these agents (1–4).

Human IgG4 molecules form bsAbs through a physiological process termed Fab-arm exchange (FAE), in which half-molecules (HL pairs) recombine with half-molecules from other IgG4 molecules (19) (Fig. 1*A*). This process occurs naturally in vivo and can be mimicked in vitro by the addition of mild reducing agents (19). The molecular determinants driving FAE in humans were identified by site-directed mutagenesis as residues S228 (19, 20), located in the IgG4 core hinge, and R409 in the IgG4 CH3 domain (21). Thus, whereas replacing either of these residues in IgG4 by their IgG1 counterpart (i.e., P228 or K409) blocked FAE both in vitro and in vivo, introducing both residues enabled IgG1 molecules to engage in FAE (21). Because breaking the covalent linkage between half-molecules is a prerequisite for FAE, residue S228 (opposed to P228) is thought to act by making the interheavy chain disulfide bonds more susceptible to reducing conditions (22). Dissociation of the noncovalently associated CH3 domains has been shown to be the rate-limiting step in the FAE reaction (23) and heavily dependent on the composition of the CH3–CH3 interface residues (24). Indeed, residue R409 decreased the CH3–CH3 interaction strength (compared with K409 in IgG1), thus enabling human IgG4 to engage in FAE (21).

Because FAE is dynamic in nature, the resulting bsAbs, with two defined specificities, only exist transiently in a polyclonal setting in vivo (20), making bispecific IgG4 unsuitable for use as a dual-targeting therapeutic. However, the mechanism of FAE represents an attractive method for creating bsAbs, potentially overcoming limitations encountered by other strategies. In this study, we describe a method for the efficient generation of stable bispecific IgG1 molecules through a process termed controlled FAE (cFAE).

Results

Matched CH3 Domains in Combination with 2-MEA–Mediated Reduction Led to Efficient bsAb Formation. We previously reported that rhesus monkey (*Macaca mulatta*) IgG4 could engage in FAE (21). In follow-up experiments, studying interspecies FAE with recombinant human and rhesus (rh)IgG4 molecules, we and others (25) observed an unexpected increase in bispecific signal, compared with intraspecies FAE, suggesting more efficient bsAb generation (Fig. S1*A*). The increase in efficiency could be harnessed in IgG1 molecules by introducing rhesus IgG4-specific CH3 residues, I350, T370, and L405 (ITL) in a human IgG1 backbone containing

Author contributions: A.F.L., J.I.M., B.E.C.G.d.G., E.T.J.v.d.B., J.N., M.D.v.K., S.V., A.K., M.J.G., P.H.C.v.B., J.S., and P.W.H.I.P. designed research; J.I.M., B.E.C.G.d.G., E.T.J.v.d.B., J.N., M.D.v.K., and A.K. performed research; B.E.C.G.d.G. contributed new reagents/analytic tools; A.F.L., J.I.M., B.E.C.G.d.G., E.T.J.v.d.B., J.N., M.D.v.K., K.S., S.V., A.K., M.J.G., P.H.C.v.B., J.G.J.v.d.W., J.S., and P.W.H.I.P. analyzed data; and A.F.L., K.S., and P.W.H.I.P. wrote the paper.

Conflict of interest statement: The authors have stock and/or warrants in Genmab.

This article is a PNAS Direct Submission.

Freely available online through the PNAS open access option.

[1]Present address: ADC Therapeutics, Chemin de la Pacottaz 1, 1806 St-Legier, Switzerland.

[2]To whom correspondence should be addressed. E-mail: p.parren@genmab.com.

This article contains supporting information online at www.pnas.org/lookup/suppl/doi:10.1073/pnas.1220145110/-/DCSupplemental.

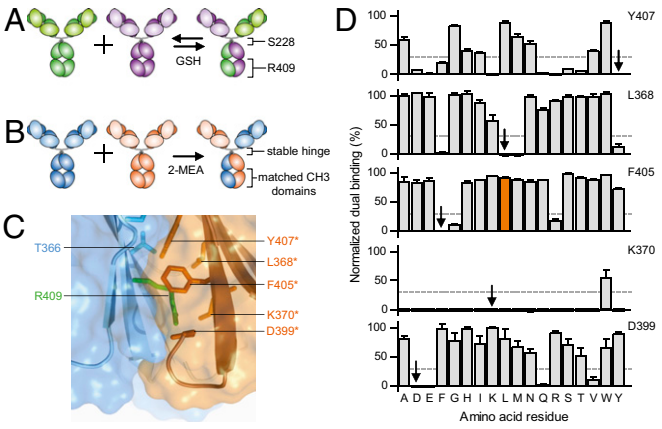

Fig. 1. Controlled Fab-arm exchange (cFAE). (*A*) Schematic representation of in vitro IgG4 Fab-arm exchange in dynamic equilibrium. IgG4 molecules containing permissive hinges (S228) and CH3 domains (R409) are incubated in the presence of reduced glutathione (GSH). (*B*) Schematic representation of in vitro generation of bsAbs by cFAE. IgG1 molecules containing stable WT hinges, and matched CH3 domain mutations are incubated in the presence of 2-MEA. (*C*) In silico model for the $CH3_{K409R}$(blue)–$CH3_{WT}$(orange) heterodimer interface. Modeling was done using PDB entry 1L6× for IgG1 Fc (28) and described previously (21). Only relevant side chains are shown in stick representation. The K409R substitution is depicted in green. Structural images were generated with PyMOL software (DeLano Scientific). (*D*) Matched CH3 mutations were identified by site-directed mutagenesis of residues Y407, L368, F405, K370, and D399. Bispecific antibodies obtained by cFAE (25 mM 2-MEA, 90 min at 37 °C) were assessed by dual-binding ELISA. Signals were normalized to that of the combination of IgG1-K409R-CD20 × IgG1-F405L-EGFR (orange bar). Residues present in WT IgG1 are indicated by arrows. Mixtures of IgG4-CD20 × IgG4-EGFR were included as reference (gray dashed line). Data represents the mean ± SEM of at least two separate experiments at a total antibody concentration of 1 μg/mL.

the P228S hinge mutation and performing FAE in combination with human IgG4 (Fig. S1*B*).

Furthermore, in a parallel effort to identify conditions that could support in vitro exchange of a stable IgG1 (i.e., P228) hinge, which intrinsically does not allow FAE in vivo (20), several reducing agents were evaluated (Fig. S2). This evaluation included 2-mercaptoethylamine-HCl (2-MEA), a mild reducing agent, which could efficiently bypass the IgG1 hinge (in the context of permissive CH3 domains) at concentrations ranging from 15 to 50 mM (which was the highest concentration examined).

Combining these two observations led to a proposed method for the generation of bsAbs, in which two IgG1s, each containing matched CH3 mutations, are produced separately and subsequently recombined by 2-MEA–mediated FAE (Fig. 1*B*). The matched CH3 mutations are required to decrease the interaction strength in both CH3 homodimers sufficiently to enable FAE, but at the same time promote more efficient CH3 heterodimerization and prevent further exchange. To find such mutations, residues L368, K370, D399, F405, and Y407, surrounding R409 in the opposite CH3 domain (Fig. 1*C*), were individually mutated (into all natural amino acids except C and P) and introduced as single point mutations into human IgG1 monoclonal antibody (HuMab) 2F8 (26), directed against epidermal growth factor receptor (EGFR). The resulting proteins were mixed with equimolar amounts of an IgG1-K409R version of HuMab 7D8 (27), directed against the CD20 antigen, and incubated for 90 min at 37 °C in PBS supplemented with 25 mM 2-MEA. After removal of 2-MEA by buffer exchange to PBS, the mixtures were assessed by means of dual-binding ELISA for their ability to support 2-MEA–mediated FAE (Fig. 1*D*). Mixtures of IgG1-F405L-EGFR [containing the CH3 determinant responsible for FAE in rhesus monkeys (21)] and IgG1-K409R-CD20 were included on each assay plate and used as reference value.

Mutating residues Y407, L368, F405, K370, or D399 resulted in numerous IgG1-EGFR point mutants that could efficiently recombine with IgG1-K409R-CD20 through 2-MEA–mediated FAE (Fig. 1*D*). Thus, a number of solutions for increased heterodimerization through FAE could be identified. Together, these results show that matched CH3 domains in combination with 2-MEA-mediated FAE can be used to efficiently generate bispecific (bs)IgG1 molecules. From here on, this process is referred to as controlled (c)FAE, and the specific combination of IgG1-K409R and IgG1-F405L was subjected to further in-depth analysis.

cFAE Is an Efficient and Flexible Process with Linear Scalability. To determine the optimal conditions for cFAE, the influence of several parameters on the generation of bsAb, from an equimolar mixture of IgG1-F405L-EGFR and IgG1-K409R-CD20 (1 mg/mL total IgG in PBS), was studied by means of dual-binding ELISA. Testing various incubation temperatures (0, 15, 25, and 37 °C) as a function of time revealed that maximal exchange, mediated by 25 mM 2-MEA, could be observed by incubating at least 60 min at 37 °C or 180 min at 25 °C (Fig. 2*A*). Varying the 2-MEA concentration (0–50 mM) during a 90-min incubation at 37 °C showed that exchange occurred at concentrations greater than 2 mM 2-MEA, and maximal exchange could be observed at concentrations of 25 mM 2-MEA and higher (Fig. 2*B*), thus confirming previous findings (Fig. S2). Under the same conditions, a mixture of IgG4-EGFR and IgG4-CD20 showed lower levels of bispecificity; however, the exchange occurred over a wider 2-MEA concentration range (Fig. 2*B*).

Electrospray ionization mass spectrometry (ESI-MS) represents a generic method to discriminate between nonexchanged parental mAbs and the resulting bsAb product with intermediate mass (20, 24). Therefore, ESI-MS was used to visualize the protein species in the samples used to generate the ELISA data in Fig. 2*B*. This analysis revealed that in accordance with the ELISA data, protein species corresponding to the parental mAbs, IgG1-F405L-EGFR and IgG1-K409R-CD20, were diminished at increasing 2-MEA concentrations, whereas the bsAb product increased accordingly (Fig. 2*B*, right *y* axis). The exchange between the corresponding IgG4 molecules resulted in ∼50% bsAb product, as expected at equilibrium with an equimolar input of parent molecules (Fig. 2*B*). Due to their overlapping molecular weight peaks, however, accurate estimation of small amounts of residual IgG1-F405L-EGFR and IgG1-K409R-CD20 homodimer species was not possible (Fig. 2*C*).

As ESI-MS data are not inherently quantitative (in addition to the peak overlap noted above), complementary methods to determine cFAE efficiency are required. Here, cation exchange chromatography (CIEX) was used to study cFAE efficiency. In the case of IgG1-F405L-EGFR and IgG1-K409R-CD20, an improved separation of parental mAbs and bsAb product enabled visualization of residual homodimers, and cFAE efficiency was shown to be 95.7% (Fig. 2*D*). To verify that cFAE can be generally applied, additional bsIgG1 molecules were prepared using additional human mAbs (Tables S1 and S2) and analyzed by CIEX (Fig. 2*E*). The results show that cFAE can be generally applied to prepare bsIgG1, and efficiencies of 94–98% can routinely be obtained.

The bench-scale cFAE process (0.1–3 mL) was further optimized for large scale, involving exchange at high IgG concentrations at ambient temperature, thus preventing the need for heating of the exchange mixture during manufacturing. For this, IgG (IgG1-F405L-EGFR and IgG1-K409R-CD20) and 2-MEA concentrations were first evaluated as a function of reaction temperature and incubation time. Exchange efficiency was determined by CIEX after removal of residual 2-MEA by gel filtration. Optimal exchange was obtained by incubation of 10 g/L of each homodimer in the presence of 50 mM 2-MEA for 5 h at 25 °C, whereas longer incubation times and higher reaction temperatures resulted in additional basic peaks (Fig. 3*A*). SDS/PAGE analysis confirmed proper assembly of bsIgG1-

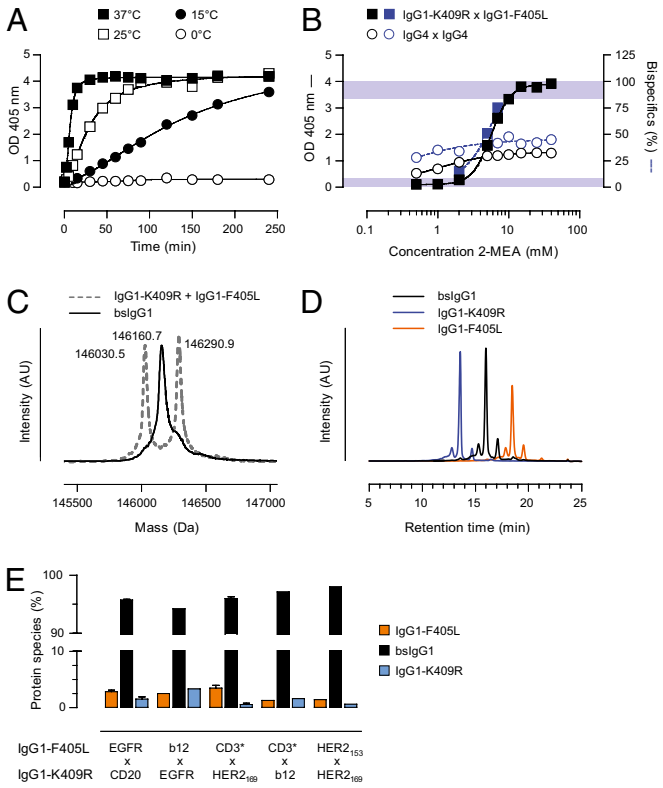

Fig. 2. Defining the conditions for cFAE. (*A*) Generation of bsAbs by cFAE (25 mM 2-MEA) at different temperatures as a function of time was assessed by dual-binding ELISA. One representative experiment is shown. Data represent dual-binding at total antibody concentrations of 1 μg/mL. (*B*) Generation of bsAbs by cFAE (90 min at 37 °C) in response to increasing 2-MEA concentrations was assessed by dual-binding ELISA (black symbols, left *y* axis) and ESI-MS (blue symbols, right *y* axis). Mixtures of IgG4 molecules (circles) were included as controls. Data represent mean ± SEM of at least two separate experiments at a total antibody concentration of 1 μg/mL. Shaded areas represent peak overlap that precludes accurate species identification by ESI-MS. (*C* and *D*) Representative deconvoluted ESI-MS spectra (*C*) and CIEX profiles (*D*) of parental mAbs and the bsAb product bsIgG1-EGFRxCD20 obtained by cFAE (25 mM 2-MEA, 90 min at 37 °C). (*E*) Matched CH3 mutations were introduced into several other human mAbs (see Tables S1 and S2 for more details), and the generation of bsAbs by cFAE (25 mM 2-MEA, 90 min at 37 °C) was monitored by CIEX.

EGFR×CD20 after 5 h at 25 °C, whereas overnight incubation resulted in more product-related impurities lacking at least one light chain (Fig. 3*B*).

The optimized conditions were subsequently scaled to a 25-L exchange reaction. The quantities of homodimers required for large-scale manufacturing were expressed using stable CHO cell lines and purified using routine unit operations commonly used for regular human IgG1. The exchange setup at 25 L was first tested using a total IgG concentration of 1 g/L, before it was run at a total IgG concentration of 20 g/L. In both cases, residual 2-MEA was removed by diafiltration. Comparison of cFAE conditions and buffer exchange at a small and large scale is shown in Table 1. The obtained exchange efficiencies of 93.0% and 94.7% were in line with the results obtained at bench scale (94.6%), showing excellent scalability of cFAE (Fig. 3*C*). Analysis of the product quality by SDS/PAGE and HP-SEC confirmed proper assembly of bsIgG1-EGFRxCD20 and the absence of aggregates (Fig. 3 *D* and *E*). Product quality was corroborated by additional biochemical analysis (Fig. S3). There was no detectable change in product quality over a 6-mo period at 5 °C (Fig. 3 *F*–*H*), demonstrating suitable in vitro stability. As expected, some degradation was observed after that period at 25 °C, and substantial degradation was observed at 40 °C. Altogether, these data convincingly show that cFAE is readily scalable.

Regular IgG1 Functional Properties Are Retained in cFAE-Derived bsIgGs. As the matched mutations are located at the CH3–CH3 interface, away from complement and Fc-receptor binding sites (28, 29), it is unlikely that IgG1 effector functions are affected. To confirm that Fc-mediated effector functions were not influenced by the matched mutations, bsIgG1-CD20×CD20 was prepared by cFAE and, together with the parental mAbs, compared with WT IgG1-CD20 for its ability to induce complement-dependent cytotoxicity (CDC) and antibody-dependent cellular cytotoxicity (ADCC). Thus, CD20-positive Daudi cells were incubated with serially diluted antibodies in the presence of human complement (CDC) or peripheral blood mononuclear cells (PBMCs) (ADCC), and cell viability was assessed by flow cytometry or ^{51}Cr-release assay, respectively. The analysis revealed no significant differences between bsIgG1-CD20×CD20, IgG1-F405L-CD20, IgG1-CD20-K409R, and WT IgG1-CD20 in the ability to lyse Daudi cells by either CDC (Fig. 4 *A* and *B*) or ADCC (Fig. 4 *C* and *D*). In contrast, bsIgG1-EGFR×CD20 was less efficient in lysing Daudi cells by CDC, probably as a result of reduced avidity due to monovalent interaction (Fig. 4*B*).

To verify that the matched mutations did not adversely affect the pharmacokinetic (PK) properties, a single dose of bsIgG1-

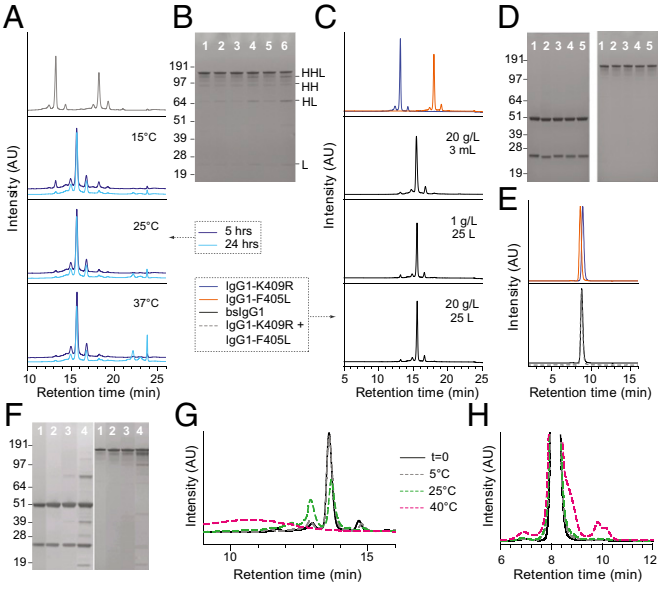

Fig. 3. Large-scale generation of bsIgG1 by cFAE. (*A*) CIEX profiles of equimolar mixtures of IgG1-EGFR-F405L and IgG1-CD20-K409R before (*Upper*) and after (*Lower*) addition of 50 mM 2-MEA and subsequent incubation at 15 °C, 25 °C, or 37 °C for 5 or 24 h. (*B*) Nonreduced SDS/PAGE of bsIgG1 batches described in *A*: 5 h at 15 °C (lane 1), 24 h at 15 °C (lane 2), 5 h at 25 °C (lane 3), 24 h at 25 °C (lane 4), 5 h at 37 °C (lane 5), and 24 h at 37 °C (lane 6). Product-related impurities resulting from loss of light (L) and heavy (H) chains are labeled on the right. (*C*) CIEX profiles of starting materials (*Upper*) and end products (*Lower*) obtained by cFAE (5 h at ambient temperature) at indicated scales. (*D*) Reduced (*Left*) and nonreduced (*Right*) SDS/PAGE of bsIgG1 batches described in *C*: IgG1-b12 assay control (lane 1), IgG1-F405L-EGFR (lane 2), IgG1-K409R-CD20 (lane 3), 25-L test run at 1 g/L (lane 4), 25-L run at 20 g/L (lane 5). (*E*) HP-SEC profiles of starting materials (*Upper*) and end product (*Lower*) of 25-L test run at 1 g/L (dashed gray line) and 25-L run at 20 g/L (solid black line). Colors correspond with *C*. (*F*–*H*) Six-month stability at 15 g/L of the heterodimer bsIgG1 (25-L run at 20 g/L) in PBS, pH 7.4, buffer at 5 °C (lane 2; gray dashed lines), 25 °C (lane 3; green dashed lines), and 40 °C (lane 4; magenta dashed lines) as assessed by reduced (*Left*) and nonreduced (*Right*) SDS/PAGE (*F*), CIEX (*G*), and HP-SEC (*H*). Reference sample (t = 0) is included (lane 1; solid black line).

Table 1. Controlled Fab-arm exchange at different scales

	Bench scale			Large scale	
Volume	0.1–0.2 mL	1–3 mL	3 mL	25 L	25 L
IgG1-2F8-F405L	0.1–0.5 g/L	0.5 g/L	10 g/L	0.5 g/L	10 g/L
IgG1-7D8-K409R	0.1–0.5 g/L	0.5 g/L	10 g/L	0.5 g/L	10 g/L
2-MEA (mM)	0–50	25	50	50	50
Reduction time	0–240 min	90 min	5 h	5 h	5 h
Temperature (°C)	15, 25, 37	37	Ambient	Ambient	Ambient
2-MEA removal	Desalting*	Desalting**	Desalting***	Diafiltration	Diafiltration
Exchange efficiency	NA	94–98%	94.60%	93.00%	94.70%
Bispecific produced	NA	NA	57.0 mg	23.25 g	473.50 g

Desalting was done by means of *spin-plate, **PD-10, or ***MicroSpin G-25 columns. NA, not assessed.

EGFR×CD20 (5 mg/kg) was injected i.v. in SCID mice and compared with a WT IgG1 PK profile. Additionally, to rule out engagement of bsIgG1 in FAE with IgG4, one group of mice received bsIgG1-EGFR×CD20 (5 mg/kg) in combination with a 10-fold excess of human IgG4 (50 mg/kg). The analysis showed that cFAE-derived bsIgG1 had a comparable PK profile to that of WT IgG1 and that this was not influenced by the presence of an excess of IgG4 (Fig. 4 *E* and *F*). Together these results show that the matched mutations had no effect on regular IgG1 effector functions and PK properties.

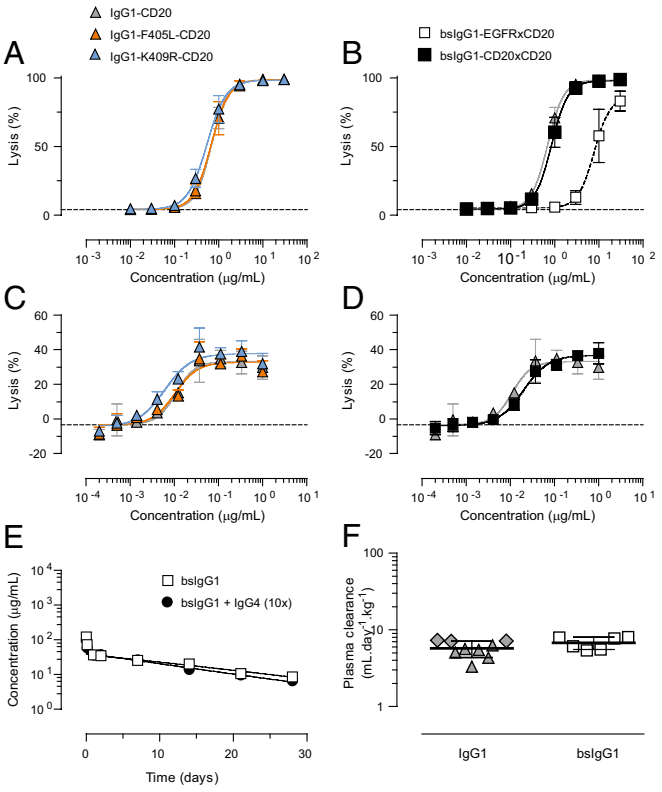

Fig. 4. Bispecific IgG1 generated by cFAE retains WT IgG1-like functionality. (*A* and *B*) CDC of Daudi cells incubated for 45 min at 37 °C with serial diluted antibodies in the presence of 20% pooled human serum. (*C* and *D*) ADCC of Daudi target cells incubated for 4 h at 37 °C with serial diluted antibodies in the presence of PBMC effector cells (E:T ratio of 100:1). Symbols correspond to *A* and *B*. (*E* and *F*) Pharmacokinetics of bsIgG1-EGFRxCD20 and WT IgG1 antibody in SCID mice. BsIgG1-EGFR×CD20 plasma concentrations were determined by dual-binding ELISA (*E*). Data represent mean concentrations ± SEM. Plasma clearance (*F*) was calculated from these data and compared with that of WT IgG1-CD20 (gray triangles) and IgG1-EGFR (gray diamonds), for which plasma concentrations were determined with antibody-specific ELISAs. Data points represent individual mice.

Efficient Tumor Killing by bsIgG1s Using Dual-Targeting Approaches Against HER2. Human epidermal growth factor receptor 2 (HER2) is a member of the EGFR family and represents a clinically well-validated target for antibody therapy (30). Besides naked (31, 32) and drug-conjugated (33) antibody approaches, HER2 is also being evaluated in dual-targeting strategies, involving (re)targeting of CD3-positive T cells to HER2-positive tumors by means of bsAbs (34, 35). Here we evaluated the in vitro and in vivo efficacy of cFAE-derived bsIgG1-N297Q-CD3×$HER2_{169}$ (Table S1).

Because simultaneous binding to both T cells and HER2-positive tumor cells is a prerequisite for T-cell (re)targeting, this was first confirmed by flow cytometry (Fig. S4 *A* and *B*). T cell–mediated cytotoxicity was assayed in vitro using AU565 target cells cocultured for 2 d with PBMCs in the presence of serial diluted bsIgG1-N297Q-CD3×$HER2_{169}$ or control antibodies. Killing of AU565 cells was then determined by measuring cell viability using alamarBlue. The results showed that, whereas control antibodies were ineffective at concentrations up to 40 μg/mL (267 nM), bsIgG1-N297Q-CD3×$HER2_{169}$ was highly effective in killing AU565 cells, with half-maximal cytotoxicity obtained at concentrations as low as 142 pg/mL (Fig. 5*A*). Moreover, T-cell activation was monitored and correlated with the observed cytotoxicity (Fig. S4 *C* and *D*).

Next, the in vivo antitumor efficacy of bsIgG1-N297Q-CD3×$HER2_{169}$ was evaluated in an adoptive transfer xenograft model, in which freshly isolated human PBMCs and NCI-N87 gastric carcinoma cells were coinjected s.c. into the flank of NOD-SCID mice. Single antibody doses ranging from 0.05 to 4 mg/kg were administered i.v. 1 h thereafter and tested in parallel to negative controls. The analysis demonstrated that doses of 0.5 or 0.05 mg/kg bsIgG1-N297Q-CD3×$HER2_{169}$ in combination with PBMCs from two separate donors were able to inhibit tumor growth compared with bsIgG1-N297Q-CD3×b12 control groups (Fig. 5 *B* and *C*). Together, these data demonstrated that bsIgG1-N297Q-CD3×$HER2_{169}$ was capable of (re)targeting T cells to HER2-positive tumor cells and induce HER2-dependent T-cell activation and tumor killing.

A second dual-targeting approach combines HER2-specific mAbs to nonoverlapping epitopes and showed enhanced antitumor effects in experimental animal models in vivo (36, 37) and in the clinic (38). Here we evaluated the efficacy of targeting two nonoverlapping HER2 epitopes by a single agent: bsIgG1-$HER2_{153}$×$HER2_{169}$. As enhanced receptor down-modulation is thought to be a key mechanism in this approach, this activity was first confirmed in vitro (Fig. S5). Next, in vivo antitumor efficacy of bsIgG1-$HER2_{153}$×$HER2_{169}$ was evaluated in a therapeutic NCI-N87 xenograft model, in which NOD-SCID mice were treated with 40 and 20 mg/kg of antibody on days 7 and 14, respectively. In this model, bsIgG1-$HER2_{153}$×$HER2_{169}$ was significantly better than the combination of IgG1-$HER2_{153}$ and IgG1-$HER2_{169}$ in inhibiting tumor growth (Fig. 5 *D* and *E*).

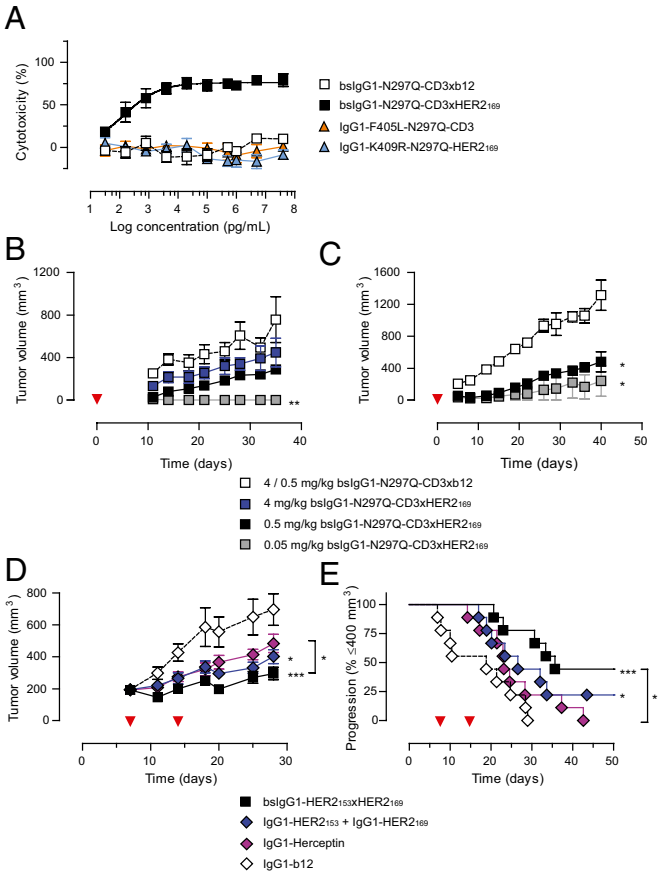

Fig. 5. Bispecific Abs show improved in vivo efficacy in selected animal models. (*A*) T cell–mediated cytotoxicity of AU565 target cells cocultured for 2 d at 37 °C with PBMC effector cells (E:T ratio 5:1) in the presence of serial diluted bsIgG1-N297Q-CD3×HER2$_{169}$. Data represent mean ± SEM of three experiments. Percentage T cells in PBMCs were 18.9%, 38.5%, and 59.8%. (*B* and *C*) Prophylactic treatment of NCI-N87 tumors in an s.c. xenograft model in NOD-SCID mice reconstituted with human PBMCs. Mice were inoculated with 5 × 10^6 NCI-N87 cells mixed with 5 × 10^6 PBMCs, randomized (n = 3–4 per group) and treated i.p. (*B*) or i.v. (*C*) 1 h thereafter. Mice receiving PBMCs from donors showing nonspecific killing of tumor cells in the absence of antibody (alloreaction) were excluded from analysis. Mice were treated with 4 mg/kg bsIgG1-N297Q-CD3×b12 or indicated doses of bsIgG1-N297Q-CD3×HER2$_{169}$, supplemented with IgG1-b12 to a total antibody dose of 4 mg/kg (*B*) or with 0.5 mg/kg bsIgG1-N297Q-CD3×b12 or indicated doses of bsIgG1-N297Q-CD3xHER2$_{169}$ (*C*). Data indicate mean tumor volumes ± SEM (red arrowheads indicate treatment days). (*D* and *E*) Treatment of established NCI-N87 tumors in an s.c. xenograft model in SCID mice. Mice were treated with a 40-mg/kg i.p. dose of total antibody on day 7, followed by a 20-mg/kg i.p. dose on day 14 (red arrowheads indicate treatment days). Data represent mean tumor volumes ± SEM (*D*) and time to progression (as defined by mice with tumor volumes ≤ 400 mm^3) (*E*). The experiment was repeated twice with similar results. Statistical significance was determined by one-way ANOVA (Tukeys multiple comparison) in *B*–*D* and by log-rank Mantel-Cox analysis in *E* (*P < 0.05; **P < 0.01; ***P < 0.001).

Discussion

Whereas most strategies to create bsAbs by design are based on genetic fusion or coexpression of two antigen binding moieties, one of nature's solutions to generate bispecificity involves the swapping of antigen binding arms (HL pairs) between individually expressed mAb molecules (19, 21, 39). Using this basic principle, we devised a method in which separately expressed mAbs efficiently recombine to form stable bsIgG1 molecules through cFAE. In this method, the recombination of antigen binding arms is driven by matched point mutations, introduced in IgG1, which weaken the noncovalent CH3–CH3 interaction enough to allow dissociation of each homodimer on reduction of the hinge disulfide bridges in vitro. At the same time, the matched point mutations strongly favor heterodimerization, thus promoting bsIgG1 end product yield and postexchange stability on reoxidation of the hinge. The use of a WT IgG1 hinge, resistant to reduction under physiological conditions in vivo (21), further adds to the postexchange stability of the bsIgG1 end product.

Mutations promoting H chain heterodimerization by various methods have been described previously by others (7, 10, 11, 40, 41). In those cases, however, multiple mutations in at least one of the H chains were required. Surprisingly, using the cFAE strategy, a matched set of single point mutations was enough to achieve at least the same level of efficiency, and multiple matching sets were identified (Figs. 1 and 2). The fact that the equilibriums involved can be controlled more precisely during in vitro exchange compared with the intracellular conditions during coexpression may have contributed to these results. As the matched mutations are few in number and located at the CH3–CH3 interface, distal from sites interacting with effector functions, it is not surprising that WT IgG1 functionality is retained in bsIgG1 (Fig. 4). Furthermore, compatibility with additional Fc modifications (e.g., N297Q) and human IgG2, IgG3, and IgG4 backbones (Fig. S6) suggests that cFAE is broadly applicable.

The major advantage of a separate expression approach is that the need for common L (or H) chains to improve product yield and homogeneity becomes superfluous while original VH-VL pairings are maintained, thus potentially increasing the exploitable repertoire of parental mAbs. An additional advantage may be that in combination with simple mixing grids for parental mAbs, high-throughput generation and screening of bsAbs become more manageable (Fig. S7), increasing the chance of discovering effective dual-targeting candidates.

Because critical steps for cFAE are compatible with routine operations for industrial production of regular human IgG1, this method appears highly suitable for large-scale manufacturing. This suitability was confirmed by large-scale implementation of the bench-scale protocol without elaborate optimization or loss of product quality (Fig. 3; Fig. S3). Additionally, potential undesired byproducts were not detected (e.g., swapped L chains), further confirming the robustness of the process, although full validation will require more detailed and sensitive analyses on a product by product basis.

Targeting T cells to HER2-positive tumors by means of bsIgG1-N297Q-CD3×HER2$_{169}$ induced HER2-dependent T-cell activation and effective tumor killing (Fig. 5; Fig. S4). Despite the presence of the N297Q mutation to preclude Fc receptor–mediated cross-linking, potentially contributing to cytokine release syndrome (42), some evidence for T-cell activation by the bsIgG1-N297Q-CD3×b12 control antibody was observed at higher concentrations (Fig. S4). This activation suggests that for this application, a (bs)IgG1-N297Q backbone may not be silent enough, as also demonstrated by others (43), and alternative nonactivating backbones should be evaluated.

The success of targeting HER2 with two distinct mAbs has been attributed to various factors, including enhanced receptor down-modulation (36, 37). In the present study, a single bsAb combining two nonoverlapping HER2 binding specificities was as effective in down-modulating HER2 in AU565 cells in vitro as the mix of parental mAbs (Fig. S5). Surprisingly, however, bsIgG1-HER2$_{153}$×HER2$_{169}$ showed superior efficacy compared with the combination of IgG1-HER2$_{153}$ and IgG1-HER2$_{169}$ in a NCI-N87 human gastric cancer xenograft model in vivo. It may thus be difficult to predict how bsAbs will act based on the antitumor mechanisms of a single or even the combination of parental mAbs. This superior activity does, however, suggest that some antibody pairs may benefit more from a bsAb approach than from a combination strategy.

In summary, using cFAE to create bsIgG1 ensures a proper in vivo half-life, intact Fc effector functions, and good manufacturability while retaining a regular IgG structure. Compatibility with

other subclasses and Fc modifications suggest that this method can be universally applied to produce bsAbs.

Materials and Methods

Parental antibodies were cloned, expressed and purified as described in *SI Materials and Methods*. The bispecific antibodies were generated by controlled Fab-arm exchange at both bench and manufacturing scale and subjected to extensive biochemical and physicochemical characterization (details in *SI Materials and Methods*). Bispecific antibodies were functionally compared to wild-type IgG1 in several in vitro and in vivo assays assessing Fc-mediated effector functions and pharmacokinetic properties (details in *SI Materials and Methods*). In vivo xenograft studies were carried out to demonstrate efficacy of bispecific antibodies in dual-targeting approaches.

ACKNOWLEDGMENTS. We thank E. Slootjes, P. Engelberts, I. Somers, M. Brandhorst, M. Chenani, and M. Voorhorst for excellent technical assistance, S. Loverix, W. Bleeker, and T. Vink for advice, and members of the SPARREN team for helpful discussions.

1. Chan AC, Carter PJ (2010) Therapeutic antibodies for autoimmunity and inflammation. *Nat Rev Immunol* 10(5):301–316.
2. Carter P (2001) Bispecific human IgG by design. *J Immunol Methods* 248(1–2):7–15.
3. Chames P, Baty D (2009) Bispecific antibodies for cancer therapy. *Curr Opin Drug Discov Devel* 12(2):276–283.
4. Kufer P, Lutterbüse R, Baeuerle PA (2004) A revival of bispecific antibodies. *Trends Biotechnol* 22(5):238–244.
5. Jackman J, et al. (2010) Development of a two-part strategy to identify a therapeutic human bispecific antibody that inhibits IgE receptor signaling. *J Biol Chem* 285(27): 20850–20859.
6. Milstein C, Cuello AC (1983) Hybrid hybridomas and their use in immunohistochemistry. *Nature* 305(5934):537–540.
7. Merchant AM, et al. (1998) An efficient route to human bispecific IgG. *Nat Biotechnol* 16(7):677–681.
8. Lindhofer H, Mocikat R, Steipe B, Thierfelder S (1995) Preferential species-restricted heavy/light chain pairing in rat/mouse quadromas. Implications for a single-step purification of bispecific antibodies. *J Immunol* 155(1):219–225.
9. Schaefer W, et al. (2011) Immunoglobulin domain crossover as a generic approach for the production of bispecific IgG antibodies. *Proc Natl Acad Sci USA* 108(27): 11187–11192.
10. Gunasekaran K, et al. (2010) Enhancing antibody Fc heterodimer formation through electrostatic steering effects: Applications to bispecific molecules and monovalent IgG. *J Biol Chem* 285(25):19637–19646.
11. Davis JH, et al. (2010) SEEDbodies: Fusion proteins based on strand-exchange engineered domain (SEED) CH3 heterodimers in an Fc analogue platform for asymmetric binders or immunofusions and bispecific antibodies. *Protein Eng Des Sel* 23(4): 195–202.
12. Wu C, et al. (2007) Simultaneous targeting of multiple disease mediators by a dual-variable-domain immunoglobulin. *Nat Biotechnol* 25(11):1290–1297.
13. Baeuerle PA, Reinhardt C (2009) Bispecific T-cell engaging antibodies for cancer therapy. *Cancer Res* 69(12):4941–4944.
14. Dimasi N, et al. (2009) The design and characterization of oligospecific antibodies for simultaneous targeting of multiple disease mediators. *J Mol Biol* 393(3):672–692.
15. Dong J, et al. (2011) A stable IgG-like bispecific antibody targeting the epidermal growth factor receptor and the type I insulin-like growth factor receptor demonstrates superior anti-tumor activity. *MAbs* 3(3):273–288.
16. Mabry R, et al. (2010) Engineering of stable bispecific antibodies targeting IL-17A and IL-23. *Protein Eng Des Sel* 23(3):115–127.
17. De Bernardis F, et al. (2007) Human domain antibodies against virulence traits of Candida albicans inhibit fungus adherence to vaginal epithelium and protect against experimental vaginal candidiasis. *J Infect Dis* 195(1):149–157.
18. Shen J, et al. (2007) Single variable domain antibody as a versatile building block for the construction of IgG-like bispecific antibodies. *J Immunol Methods* 318(1–2):65–74.
19. van der Neut Kolfschoten M, et al. (2007) Anti-inflammatory activity of human IgG4 antibodies by dynamic Fab arm exchange. *Science* 317(5844):1554–1557.
20. Labrijn AF, et al. (2009) Therapeutic IgG4 antibodies engage in Fab-arm exchange with endogenous human IgG4 in vivo. *Nat Biotechnol* 27(8):767–771.
21. Labrijn AF, et al. (2011) Species-specific determinants in the IgG CH3 domain enable Fab-arm exchange by affecting the noncovalent CH3-CH3 interaction strength. *J Immunol* 187(6):3238–3246.
22. Bloom JW, Madanat MS, Marriott D, Wong T, Chan SY (1997) Intrachain disulfide bond in the core hinge region of human IgG4. *Protein Sci* 6(2):407–415.
23. Rispens T, Ooijevaar-de Heer P, Bende O, Aalberse RC (2011) Mechanism of immunoglobulin G4 Fab-arm exchange. *J Am Chem Soc* 133(26):10302–10311.
24. Rose RJ, et al. (2011) Quantitative analysis of the interaction strength and dynamics of human IgG4 half molecules by native mass spectrometry. *Structure* 19(9):1274–1282.
25. Warncke M, et al. (2012) Different adaptations of IgG effector function in human and nonhuman primates and implications for therapeutic antibody treatment. *J Immunol* 188(9):4405–4411.
26. Bleeker WK, et al. (2004) Dual mode of action of a human anti-epidermal growth factor receptor monoclonal antibody for cancer therapy. *J Immunol* 173(7):4699–4707.
27. Teeling JL, et al. (2004) Characterization of new human CD20 monoclonal antibodies with potent cytolytic activity against non-Hodgkin lymphomas. *Blood* 104(6): 1793–1800.
28. Idusogie EE, et al. (2000) Mapping of the C1q binding site on rituxan, a chimeric antibody with a human IgG1 Fc. *J Immunol* 164(8):4178–4184.
29. Shields RL, et al. (2001) High resolution mapping of the binding site on human IgG1 for Fc gamma RI, Fc gamma RII, Fc gamma RIII, and FcRn and design of IgG1 variants with improved binding to the Fc gamma R. *J Biol Chem* 276(9):6591–6604.
30. Hurvitz SA, Hu Y, O'Brien N, Finn RS (2013) Current approaches and future directions in the treatment of HER2-positive breast cancer. *Cancer Treat Rev* 39(3):219–229.
31. Adams CW, et al. (2006) Humanization of a recombinant monoclonal antibody to produce a therapeutic HER dimerization inhibitor, pertuzumab. *Cancer Immunol Immunother* 55(6):717–727.
32. Slamon DJ, et al. (2001) Use of chemotherapy plus a monoclonal antibody against HER2 for metastatic breast cancer that overexpresses HER2. *N Engl J Med* 344(11): 783–792.
33. Lewis Phillips GD, et al. (2008) Targeting HER2-positive breast cancer with trastuzumab-DM1, an antibody-cytotoxic drug conjugate. *Cancer Res* 68(22):9280–9290.
34. Davol PA, Smith JA, Kouttab N, Elfenbein GJ, Lum LG (2004) Anti-CD3 x anti-HER2 bispecific antibody effectively redirects armed T cells to inhibit tumor development and growth in hormone-refractory prostate cancer-bearing severe combined immunodeficient beige mice. *Clin Prostate Cancer* 3(2):112–121.
35. Jäger M, Schoberth A, Ruf P, Hess J, Lindhofer H (2009) The trifunctional antibody ertumaxomab destroys tumor cells that express low levels of human epidermal growth factor receptor 2. *Cancer Res* 69(10):4270–4276.
36. Ben-Kasus T, Schechter B, Lavi S, Yarden Y, Sela M (2009) Persistent elimination of ErbB-2/HER2-overexpressing tumors using combinations of monoclonal antibodies: Relevance of receptor endocytosis. *Proc Natl Acad Sci USA* 106(9):3294–3299.
37. Friedman LM, et al. (2005) Synergistic down-regulation of receptor tyrosine kinases by combinations of mAbs: Implications for cancer immunotherapy. *Proc Natl Acad Sci USA* 102(6):1915–1920.
38. Baselga J, et al.; CLEOPATRA Study Group (2012) Pertuzumab plus trastuzumab plus docetaxel for metastatic breast cancer. *N Engl J Med* 366(2):109–119.
39. Schuurman J, et al. (1999) Normal human immunoglobulin G4 is bispecific: It has two different antigen-combining sites. *Immunology* 97(4):693–698.
40. Moore GL, et al. (2011) A novel bispecific antibody format enables simultaneous bivalent and monovalent co-engagement of distinct target antigens. *MAbs* 3(6):546–557.
41. Strop P, et al. (2012) Generating bispecific human IgG1 and IgG2 antibodies from any antibody pair. *J Mol Biol* 420(3):204–219.
42. Wing MG, et al. (1996) Mechanism of first-dose cytokine-release syndrome by CAMPATH 1-H: Involvement of CD16 (FcgammaRIII) and CD11a/CD18 (LFA-1) on NK cells. *J Clin Invest* 98(12):2819–2826.
43. Nesspor TC, Raju TS, Chin CN, Vafa O, Brezski RJ (2012) Avidity confers FcγR binding and immune effector function to aglycosylated immunoglobulin G1. *J Mol Recognit* 25(3):147–154.